International Journal of Control and Automation
Vol. 8, No. 9 (2015), pp. 139-152
http://dx.doi.org/10.14257/ijca.2015.8.9.14

Distributed Containment Control for Multi-robot System Based on Binocular Vision and RBF Neural Network

Nuan Shao, Huiguang Li, Le Liu and Guoyou Li

Key Lab of Industrial Computer Control Engineering of Hebei Province, College of Electrical Engineering, Yanshan University, Qinhuangdao 066004, China
shaonuan@ysu.edu.cn, ydlihuiguang@163.com,
leliu@ysu.edu.cn, lgyysu@163.com

Abstract

Aiming at the distributed containment control problem for multi-robot system with dynamic leaders, we use binocular vision as the sensing device, so firstly, a binocular visual model for dynamic target is established by introducing the pseudo depth variable, and it is used to provide real-time status information for the followers. Then, in the case that each follower can only get information from part of the leaders, even individual follower can not get any information from the leaders directly, the topological relationship among robots is built by using the graph theory. Once more, RBF neural networks are employed to approximate the uncertainties in the system model of followers, and L_2 *robust control laws are used to restrain the influences of the approximation errors. Finally, a simulation is carried out on multiple 2 degrees-of-freedom (DOF) robots, and results validate the designed controllers can drive the followers converge to the convex hull spanned by the leaders asymptotically and realize synchronization motion ultimately.*

Keywords: *multi-robot system, distributed containment control, binocular visual servo control, RBF neural network*

1. Introduction

Due to the higher robustness, less communication cost, and greater efficiency, distributed control of multi-agent system has attracted a considerable amount of attention in recent years [1], in which leader-following problem is a major focal point. In [2], when the system exist a dynamic virtual leader, and a variable structure method is designed to solve the distributed coordinated tracking problem. Reference [3] studies the distributed containment control problem for double-integrator dynamics in the presence of both stationary and dynamic leaders. References [1, 4] focus on consensus for a group of agents without any leader.

With the rapid development of distributed control of multi-agent system, the containment control of networked Lagrange systems is receiving significant attention recently. For instance, [5] studies the swarm tracking control problem for a set of Lagrange systems, and the controllers are designed by considering leaders' generalized

ISSN: 2005-4297 IJCA

coordinate derivatives are respectively, constant and time-varying. In [6], for the networked Lagrange systems with multiple dynamic leaders in the presence of parametric uncertainties under a directed graph, a distributed adaptive control algorithm combined with distributed sliding-mode estimator is proposed. In [7], the distributed coordination control problem without using neighbors' velocity information in the absence of communication with multiple stationary leaders and the leaderless is considered.

Although there are many results on containment control of multi-agent system, but we can find that the visual sensor has not been widely used in this area as a communication device. Using visual sensor need to solve the problem of image Jacobian matrix firstly, which is the mapping matrix between image feature space and robot operating space, and it is the key to the visual servo operation. For the monocular visual servo system, the distance from the camera to the object (depth) can not be obtained directly, and this is an urgent problem in solving image Jacobian matrix. A large number of literatures adopt the method of approximate calculating or online estimation to solve this problem, but parameter estimation error tend to make the robot control task can not be achieved. In addition, a depth-independent interaction matrix is proposed in [8], which is different from the traditional interaction matrix because it does not need obtain the depth information of the feature point, but the controller design is relatively complex due to the presence of regression matrix. By contrast, the binocular visual system can avoid this problem due to the existence of the parallax. In [9], two cameras are installed in parallel and a binocular visual servoing model is proposed for static target. Afterward this model is applied into the eye-in-hand robot visual servo control system [10] and the design of speed observer [11], and both of the applications can achieve favorable control performance.

In this paper, based on the visual structure which is proposed in [9], we establish a binocular visual model for dynamic target, so it can provide real-time status information for the followers. Once more, distributed containment controllers for multi-robot system are designed by using the sliding mode control method and RBF neural networks, in which RBF neural networks are adopted to approximate the unknown nonlinear functions, and L_2 robust control laws are used to restrain the influences of the approximation errors. Finally, a simulation research is carried out on multiple 2-DOF robots to show the effectiveness of the proposed control algorithms.

2. System Description and Graph Theory

Each robot is taken as an agent in this paper. We consider a team of m followers, labeled as robots 1 to m, and $n-m\,(n>m)$ leaders labeled as robots $m+1$ to n. The followers system are described as more realistic nonlinear Euler-Lagrange dynamics

$$\boldsymbol{M}_i(\boldsymbol{q}_i)\ddot{\boldsymbol{q}}_i + \boldsymbol{C}_i(\boldsymbol{q}_i,\dot{\boldsymbol{q}}_i)\dot{\boldsymbol{q}}_i + \boldsymbol{G}_i(\boldsymbol{q}_i) + \boldsymbol{d}_i + \boldsymbol{\tau}_{di} = \boldsymbol{\tau}_i,\quad i = 1,\ldots,m \tag{1}$$

where $\boldsymbol{M}_i \in \mathbf{R}^{p\times p}$ is the symmetric positive-definite inertia matrix, $\boldsymbol{C}_i \in \mathbf{R}^{p\times p}$ is the

vector of Coriolis and centrifugal torques, $\boldsymbol{G}_i \in \mathbf{R}^{p\times 1}$ is the vector of gravitational torques, $\boldsymbol{d}_i \in \mathbf{R}^{p\times 1}$ is the system modeling error, $\boldsymbol{\tau}_{di} \in \mathbf{R}^{p\times 1}$ is the vector of external disturbances and $\boldsymbol{\tau}_i \in \mathbf{R}^{p\times 1}$ is the control force.

The information flow among the robots (both followers and leaders) can be described by using a directed graph $\boldsymbol{G} = (\boldsymbol{V}, \boldsymbol{\varepsilon})$, in which $\boldsymbol{V}$ is the finite non-empty set of nodes, and $\boldsymbol{\varepsilon} \subseteq \boldsymbol{V} \times \boldsymbol{V}$ is the edge set. In this paper, the follower set and the leader set are respectively denoted as $\boldsymbol{F} := \{V_1, V_2, \cdots, V_m\}$ and $\boldsymbol{L} := \{V_{m+1}, V_{m+2}, \cdots, V_n\}$. An edge $(V_i, V_j) \in \boldsymbol{\varepsilon}$ denotes that robot j can obtain information from robot i. A sequence of the form $(V_{i1}, V_{i2}), \quad (V_{i2}, V_{i3}), \ldots$ is called a directed path.

The adjacency matrix $\boldsymbol{A} = (a_{ij}) \in \mathbf{R}^{n\times n}$ of graph $\boldsymbol{G}$ is defined as $a_{ij} > 0$ if $(V_j, V_i) \in \boldsymbol{\varepsilon}$, otherwise, $a_{ij} = 0$; self-edges are not allowed, *i.e.*, $a_{ii} = 0$. The Laplacian matrix $\boldsymbol{L}_A = [l_{ij}] \in \mathbf{R}^{n\times n}$ associated with $\boldsymbol{A}$ is defined as $l_{ii} = \sum_{j=1, j\neq i}^{n} a_{ij}$ and $l_{ij} = -a_{ij}$, $i \neq j$.

By expanding the Kronecker product [5], we have

$$(\boldsymbol{L}_A \otimes \boldsymbol{I}_p)\begin{bmatrix}\boldsymbol{x}_F\\ \boldsymbol{x}_L\end{bmatrix} = \begin{bmatrix}\boldsymbol{L}_1 \otimes \boldsymbol{I}_p & \boldsymbol{L}_2 \otimes \boldsymbol{I}_p\\ \boldsymbol{0}_{p(n-m)\times m} & \boldsymbol{0}_{p(n-m)\times(n-m)}\end{bmatrix}\begin{bmatrix}\boldsymbol{x}_F\\ \boldsymbol{x}_L\end{bmatrix} \tag{2}$$

where $\boldsymbol{x}_F = \left[x_1^T, x_2^T, \ldots, x_m^T\right]^T$ represents the generalized coordinates of the followers, and $\boldsymbol{x}_L = \left[x_{m+1}^T, x_{m+2}^T, \ldots, x_n^T\right]^T$ represents the generalized coordinates of the leaders, $\boldsymbol{L}_1 \in \mathbf{R}^{m\times m}$, $\boldsymbol{L}_2 \in \mathbf{R}^{m\times(n-m)}$.

Definition 1 [6]: Let $\boldsymbol{Q}$ be a set in a real vector space $\boldsymbol{V} \in \mathbf{R}^{n\times 1}$. The set $\boldsymbol{Q}$ is convex if, for any x and y in $\boldsymbol{Q}$, the point $(1-\kappa)x + \kappa y \in \boldsymbol{Q}$ for any $\kappa \in [0, 1]$. The convex hull for a set of points $\boldsymbol{X} = \{x_1, \cdots, x_n\}$ in $\boldsymbol{V}$ is the minimal convex set containing all points in $\boldsymbol{X}$, and we can use $co\{\boldsymbol{X}\}$ to denote it.

Lemma 1 [5]: For each follower, if there exists at least one leader that has a directed path to this follower, then $\boldsymbol{L}_1$ in (2) is positive-definite. In addition, each entry of $-\boldsymbol{L}_1^{-1}\boldsymbol{L}_2$ is nonnegative and the sum of each row of $-\boldsymbol{L}_1^{-1}\boldsymbol{L}_2$ is equal to one. This further shows that $-\left(\boldsymbol{L}_1^{-1}\boldsymbol{L}_2 \otimes \boldsymbol{I}_P\right)\boldsymbol{x}_L \in co\left\{x_j, j \in \boldsymbol{L}\right\}$.

3. Binocular Visual Servo Model

According to the visual structure in [9], the relationship between the camera coordinate system $X_C - Y_C - Z_C$ and the image coordinate system $x - y$ can be expressed as follows

$$\begin{cases} X_C = \dfrac{x_1}{x_1 - x_2} B \\ Y_C = \dfrac{y}{x_1 - x_2} B \\ Z_C = \dfrac{f}{x_1 - x_2} B \end{cases} \tag{3}$$

where (x_1, y) and (x_2, y) are the image coordinates in the left and right camera, respectively; B is the distance between the optical centers of two camera lenses; f is the focal length.

Define $\boldsymbol{u}^C = [T_{XC} \quad T_{YC} \quad T_{ZC} \quad \omega_{XC} \quad \omega_{YC} \quad \omega_{ZC}]^{\mathrm{T}}$ represent the end-effector velocities in the camera coordinate system and $\boldsymbol{v}_o^C = [T_{OX} \quad T_{OY} \quad T_{OZ}]^{\mathrm{T}}$ represent the object point velocities in camera coordinate system, then the next relationship holds

$$\begin{bmatrix} \dot{X}_C \\ \dot{Y}_C \\ \dot{Z}_C \end{bmatrix} = \begin{bmatrix} -1 & 0 & 0 & 0 & -Z_C & Y_C \\ 0 & -1 & 0 & Z_C & 0 & -X_C \\ 0 & 0 & -1 & -Y_C & X_C & 0 \end{bmatrix} \begin{bmatrix} T_{XC} \\ T_{YC} \\ T_{ZC} \\ \omega_{XC} \\ \omega_{YC} \\ \omega_{ZC} \end{bmatrix} + \begin{bmatrix} T_{OX} \\ T_{OY} \\ T_{OZ} \end{bmatrix} \tag{4}$$

Take the pseudo depth variable $\sigma = x_1 - x_2$, and substituting (3) into (4), then the binocular visual servo control model can be expressed as

$$\underbrace{\begin{bmatrix} \dot{x}_1 \\ \dot{y} \\ \dot{\sigma} \end{bmatrix}}_{\dot{\boldsymbol{m}}} = \underbrace{\begin{bmatrix} -\dfrac{\sigma}{B} & 0 & \dfrac{x_1\sigma}{fB} & \dfrac{x_1 y}{f} & -\dfrac{f^2 + x_1^2}{f} & y \\ 0 & -\dfrac{\sigma}{B} & \dfrac{y\sigma}{fB} & \dfrac{f^2 + y^2}{f} & -\dfrac{x_1 y}{f} & -x_1 \\ 0 & 0 & \dfrac{\sigma^2}{fB} & \dfrac{y\sigma}{f} & -\dfrac{x_1\sigma}{f} & 0 \end{bmatrix}}_{\boldsymbol{J}_{image}} \underbrace{\begin{bmatrix} T_{XC} \\ T_{YC} \\ T_{ZC} \\ \omega_{XC} \\ \omega_{YC} \\ \omega_{ZC} \end{bmatrix}}_{\boldsymbol{u}^C} + \underbrace{\begin{bmatrix} \dfrac{\sigma}{B} & 0 & -\dfrac{x_1\sigma}{fB} \\ 0 & \dfrac{\sigma}{B} & -\dfrac{y\sigma}{fB} \\ 0 & 0 & -\dfrac{\sigma^2}{fB} \end{bmatrix}}_{\boldsymbol{J}_0} \underbrace{\begin{bmatrix} T_{OX} \\ T_{OY} \\ T_{OZ} \end{bmatrix}}_{\boldsymbol{v}_O^C} \tag{5}$$

where x_1, y and σ can be derived from the coordinates of the object point in the image plane, and then the parameters of this image Jacobian matrix J_{image} can be calculated in real-time, thereby avoiding the estimation of the depth information. The pseudo depth variable σ is only varies inversely as the depth information, i.e., its value is larger, the distance between the object point and the camera is closer, and vice versa.

4. Distributed Containment Control for Multi-robot System with Dynamic Leaders

4.1. Design of Sliding Mode Controller Based on Binocular Vision

Under the constructed directed topological relationship, each follower can obtain a target point according to the real-time status information of its neighbor robots (part of the

leaders or other followers in its view), and the target point will guide the movement of the corresponding follower as the desired state signal. If we combine (3) with the directed graph of graph theory, then the target point's position of follower i in the camera coordinate system can be calculated by

$$\boldsymbol{C}_i = \begin{bmatrix} X_{C_i} & Y_{C_i} & Z_{C_i} \end{bmatrix}^{\mathrm{T}} = \frac{1}{\sum_{j=1, j\neq i}^{n} a_{ij}} \sum_{j=1, j\neq i}^{n} \left[\left(a_{ij} \otimes \boldsymbol{I}_p \right) \boldsymbol{C}_j^i \right] \tag{6}$$

where $\boldsymbol{C}_j^i = \begin{bmatrix} \dfrac{Bx_{1j}^i}{\left(x_{1j}^i - x_{2j}^i\right)} & \dfrac{By_j^i}{\left(x_{1j}^i - x_{2j}^i\right)} & \dfrac{fB}{\left(x_{1j}^i - x_{2j}^i\right)} \end{bmatrix}^{\mathrm{T}}$, and it can be obtained by using the real-time coordinate values $\left(x_{1j}^i, y_j^i\right)$ and $\left(x_{2j}^i, y_j^i\right)$ of robot j in the image plane of follower i; a_{ij} is the (i, j) th entry of adjacency matrix $\boldsymbol{A}$.

Substituting (6) into (3), and then we can get the real-time image characteristics of target point of follower i

$$\boldsymbol{m}_i = \begin{bmatrix} \dfrac{fX_{C_i}}{Z_{C_i}} & \dfrac{fY_{C_i}}{Z_{C_i}} & \dfrac{fB}{Z_{C_i}} \end{bmatrix}^{\mathrm{T}} \tag{7}$$

Suppose the intrinsic parameters of the cameras are known, and according to the differential kinematics of a robotic manipulator in [12], the relationship between the joint velocities $\dot{\boldsymbol{q}}_i$ and the end-effector velocities $\boldsymbol{u}_i^{C_i}$ in the camera coordinate system can be described as

$$\boldsymbol{u}_i^{C_i} = \begin{bmatrix} \boldsymbol{R}_{B_i}^{C_i} & \boldsymbol{0} \\ \boldsymbol{0} & \boldsymbol{R}_{B_i}^{C_i} \end{bmatrix} \begin{bmatrix} \mathbf{I} & \boldsymbol{0} \\ \boldsymbol{0} & \boldsymbol{T}(\boldsymbol{q}_i) \end{bmatrix} \boldsymbol{J}_A(\boldsymbol{q}_i) \dot{\boldsymbol{q}}_i \tag{8}$$

where $\boldsymbol{R}_{B_i}^{C_i}$ is the rotation matrix of the base coordinate system with respect to the camera coordinate system of follower i, $\boldsymbol{T}(\boldsymbol{q}_i)$ is the transformation matrix that depends on the parameterization of the end-effector orientation, $\boldsymbol{J}_A(\boldsymbol{q}_i)$ is the analytical Jacobian matrix which is possible to computed the Jacobian matrix via differentiation of the direct kinematics with respect to the joint positions.

Combine (5) and (8) together, then the target point's velocities of follower i in the image plane coordinate system can be written as

$$\dot{\boldsymbol{m}}_i = \boldsymbol{J}_{image_i} \begin{bmatrix} \boldsymbol{R}_{B_i}^{C_i} & \boldsymbol{0} \\ \boldsymbol{0} & \boldsymbol{R}_{B_i}^{C_i} \end{bmatrix} \begin{bmatrix} \mathbf{I} & \boldsymbol{0} \\ \boldsymbol{0} & \boldsymbol{T}(\boldsymbol{q}_i) \end{bmatrix} \boldsymbol{J}_A(\boldsymbol{q}_i) \dot{\boldsymbol{q}}_i + \boldsymbol{J}_{0_i} \boldsymbol{V}_{O_i}^{C_i} \tag{9}$$

Further, (9) can be abbreviated as

$$\dot{\boldsymbol{m}}_i = \boldsymbol{J}_i(\boldsymbol{q}_i, \boldsymbol{m}_i) \dot{\boldsymbol{q}}_i + \boldsymbol{J}_{0_i} \boldsymbol{V}_{O_i}^{C_i} \tag{10}$$

where $\boldsymbol{J}_i(\boldsymbol{q}_i, \boldsymbol{m}_i) = \boldsymbol{J}_{image_i} \begin{bmatrix} \boldsymbol{R}_{B_i}^{C_i} & \boldsymbol{0} \\ \boldsymbol{0} & \boldsymbol{R}_{B_i}^{C_i} \end{bmatrix} \begin{bmatrix} \mathbf{I} & \boldsymbol{0} \\ \boldsymbol{0} & \boldsymbol{T}(\boldsymbol{q}_i) \end{bmatrix} \boldsymbol{J}_A(\boldsymbol{q}_i)$ is called the robot Jacobian matrix hereafter in this paper.

In this section, we adopt the image-based visual servo control method, and for the target point of follower i, its image feature error between the real-time image feature $\boldsymbol{m}_i$

and the desired image feature $\boldsymbol{m}_{di}$ can be defined as $\boldsymbol{e}_i = \boldsymbol{m}_{di} - \boldsymbol{m}_i$, thus the control problem is to design a distributed containment control algorithm to ensure $\lim_{t\to\infty} \boldsymbol{e}_i(t) = 0$, such that all followers converge to the convex hull spanned by the dynamic leaders asymptotically.

Before moving on, the sliding mode surface and the actual reference trajectory are, respectively, given by

$$\boldsymbol{s}_i = \dot{\boldsymbol{q}}_i + \boldsymbol{J}_i^{+}\boldsymbol{J}_{0_i}\boldsymbol{V}_{O_i}^{C_i} - \boldsymbol{J}_i^{+}\boldsymbol{\Lambda}\boldsymbol{e}_i \tag{11}$$

$$\dot{\boldsymbol{q}}_{ri} = -\boldsymbol{J}_i^{+}\boldsymbol{J}_{0_i}\boldsymbol{V}_{O_i}^{C_i} + \boldsymbol{J}_i^{+}\boldsymbol{\Lambda}\boldsymbol{e}_i \tag{12}$$

Take the time derivative of $\boldsymbol{s}_i$, and we can get

$$\begin{aligned}\boldsymbol{M}_i\dot{\boldsymbol{s}}_i &= -\boldsymbol{M}_i\ddot{\boldsymbol{q}}_{ri} + (\boldsymbol{\tau}_i - \boldsymbol{C}_i\dot{\boldsymbol{q}}_i - \boldsymbol{G}_i - \boldsymbol{\tau}_{di} - \boldsymbol{d}_i) \\ &= -(\boldsymbol{M}_i\ddot{\boldsymbol{q}}_{ri} + \boldsymbol{C}_i\dot{\boldsymbol{q}}_{ri} + \boldsymbol{G}_i) + \boldsymbol{\tau}_i - \boldsymbol{C}_i\boldsymbol{s}_i - \boldsymbol{\omega}_i\end{aligned} \tag{13}$$

where $\boldsymbol{\omega}_i = \boldsymbol{d}_i + \boldsymbol{\tau}_{di}$ is the unknown nonlinear function, and the controller $\boldsymbol{\tau}_i$ can be preliminarily designed as

$$\boldsymbol{\tau}_i = \boldsymbol{M}_i\ddot{\boldsymbol{q}}_{ri} + \boldsymbol{C}_i\dot{\boldsymbol{q}}_{ri} + \boldsymbol{G}_i + \boldsymbol{\omega}_i - K_v\boldsymbol{s}_i \tag{14}$$

where $K_v \in \mathbf{R}^{+}$.

4.2. Approximation of RBF Neural Network

In order to improve the control precision of multi-robot system, RBF neural network is adopted to conduct approximation for the unknown nonlinear function $\boldsymbol{\omega}_i = [\omega_{i1}, \cdots, \omega_{ip}]^{\mathrm{T}}$ in (14). Structure diagram of RBF neural network is shown as Figure 1.

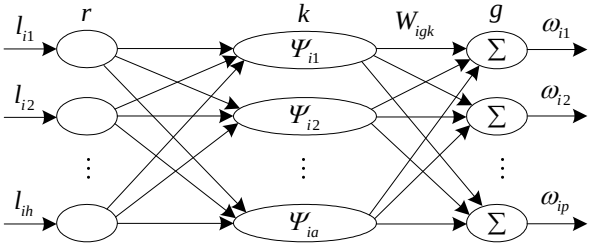

Figure 1. Structure Diagram of RBF Neural Network

In Figure 1, $\boldsymbol{I}_i = [I_{i1}, \cdots, I_{ih}]^{\mathrm{T}}$ is the input vector; $\boldsymbol{W}_i = [\boldsymbol{W}_{i1}, \cdots, \boldsymbol{W}_{ip}]^{\mathrm{T}}$ is the weight vector, and $\boldsymbol{W}_{ig} = [W_{ig1}, \cdots, W_{iga}]$; $\boldsymbol{\Psi}_i = [\Psi_{i1}, \cdots, \Psi_{ia}]^{\mathrm{T}}$ is the radial basis vector in hidden layer, and Ψ_{ik} is Gauss function

$$\Psi_{ik} = \exp\left(-\frac{\|\boldsymbol{I}_i - \boldsymbol{c}_{ik}\|}{2b_{ik}^2}\right) \tag{15}$$

where $\boldsymbol{c}_{ik} = [c_{ik1}, \cdots, c_{ikh}]$ is the centric vector of node k; $\boldsymbol{b}_i = [b_{i1}, \cdots, b_{ia}]$ is the basis

breadth vector, and b_{ik} is the basis breadth parameter of node k; $r = 1, \cdots, h$, $k = 1, \cdots, a$, $g = 1, \cdots, p$.

According to the RBF neural network approximation theory, there exists optimal RBF neural network $\boldsymbol{W}_i^{*\mathrm{T}} \boldsymbol{\Psi}_i(\boldsymbol{l}_i, \boldsymbol{c}_i, \boldsymbol{b}_i)$, which satisfies

$$\boldsymbol{\omega}_i = \boldsymbol{W}_i^{*\mathrm{T}} \boldsymbol{\Psi}_i(\boldsymbol{l}_i, \boldsymbol{c}_i, \boldsymbol{b}_i) + \boldsymbol{\varepsilon}_i \tag{16}$$

where $\boldsymbol{\varepsilon}_i$ is the approximation error. Take $\boldsymbol{\varepsilon}_i$ as external disturbance, and L_2 robust control law can be used to restrain its influence.

Theorem 1: For the robotic system (1), if we choose the parameter adaptive laws of RBF

$$\dot{\hat{\boldsymbol{W}}}_i = -\eta_i \boldsymbol{s}_i \boldsymbol{\Psi}_i^{\mathrm{T}} \tag{17}$$

Design the distributed containment controller

$$\boldsymbol{\tau}_i = \boldsymbol{M}_i \ddot{\boldsymbol{q}}_{ri} + \boldsymbol{C}_i \dot{\boldsymbol{q}}_{ri} + \boldsymbol{G}_i + \hat{\boldsymbol{W}}_i^{\mathrm{T}} \boldsymbol{\Psi} - \frac{1}{2\gamma_i^2} \boldsymbol{s}_i - K_v \boldsymbol{s}_i \tag{18}$$

Define evaluation signal $\boldsymbol{z}_i = \xi_i \boldsymbol{s}_i$, and parameter ξ_i satisfies

$$K_v - \frac{1}{2}\xi_i^2 = \varepsilon_1 \tag{19}$$

Then L_2 gain of the system is $J_R = \sup_{\|\boldsymbol{\varepsilon}_i\| \neq 0} \frac{\|\boldsymbol{z}_i\|_2}{\|\boldsymbol{\varepsilon}_i\|_2} < \gamma_i$.

Proof: Considering the following Lyapunov function candidate as

$$V = \frac{1}{2}\boldsymbol{s}_i^{\mathrm{T}} \boldsymbol{M}_i \boldsymbol{s}_i + \frac{1}{2\eta_i} tr(\tilde{\boldsymbol{W}}_i^{\mathrm{T}} \tilde{\boldsymbol{W}}_i) \tag{20}$$

where $\tilde{\boldsymbol{W}}_i = \hat{\boldsymbol{W}}_i - \boldsymbol{W}_i^*$.

Take the time derivative of (20), and then we have

$$\dot{V} = \boldsymbol{s}_i^{\mathrm{T}} \boldsymbol{M}_i \dot{\boldsymbol{s}}_i + \frac{1}{2}\boldsymbol{s}_i^{\mathrm{T}} \dot{\boldsymbol{M}}_i \boldsymbol{s}_i + \frac{1}{\eta_i} tr(\tilde{\boldsymbol{W}}_i^{\mathrm{T}} \dot{\tilde{\boldsymbol{W}}}_i) \tag{21}$$

Substituting (13), (16) and (18) into (21) yields

$$\dot{V} = \boldsymbol{s}_i^{\mathrm{T}} \tilde{\boldsymbol{W}}_i^{\mathrm{T}} \boldsymbol{\Psi}_i - \frac{1}{2\gamma_i^2} \boldsymbol{s}_i^{\mathrm{T}} \boldsymbol{s}_i - K_v \boldsymbol{s}_i^{\mathrm{T}} \boldsymbol{s}_i - \boldsymbol{s}_i^{\mathrm{T}} \boldsymbol{\varepsilon}_i + \frac{1}{\eta_i} tr(\tilde{\boldsymbol{W}}_i^{\mathrm{T}} \dot{\tilde{\boldsymbol{W}}}_i) \tag{22}$$

Define

$$H = \dot{V} - \frac{1}{2}\gamma_i^2 \|\boldsymbol{\varepsilon}_i\|^2 + \frac{1}{2}\|\boldsymbol{z}_i\|^2 \tag{23}$$

Substituting (22) into (23) yields

$$H = \boldsymbol{s}_i^{\mathrm{T}} \tilde{\boldsymbol{W}}_i^{\mathrm{T}} \boldsymbol{\Psi}_i - \boldsymbol{s}_i^{\mathrm{T}} \boldsymbol{\varepsilon}_i - \frac{1}{2\gamma_i^2} \boldsymbol{s}_i^{\mathrm{T}} \boldsymbol{s}_i - \frac{1}{2}\gamma_i^2 \|\boldsymbol{\varepsilon}_i\|^2 - K_v \boldsymbol{s}_i^{\mathrm{T}} \boldsymbol{s}_i + \frac{1}{\eta_i} tr(\tilde{\boldsymbol{W}}_i^{\mathrm{T}} \dot{\tilde{\boldsymbol{W}}}_i) + \frac{1}{2}\|\boldsymbol{z}_i\|^2 \tag{24}$$

Owing to $-\boldsymbol{s}_i^{\mathrm{T}} \boldsymbol{\varepsilon}_i - \frac{1}{2\gamma_i^2} \boldsymbol{s}_i^{\mathrm{T}} \boldsymbol{s}_i - \frac{1}{2}\gamma_i^2 \|\boldsymbol{\varepsilon}_i\|^2 = -\frac{1}{2}\left\| \frac{1}{\gamma_i} \boldsymbol{s}_i + \gamma_i \boldsymbol{\varepsilon}_i \right\|^2 \leq 0$, then we can get

$$\begin{aligned} H &\le \boldsymbol{s}_i^{\mathrm{T}} \tilde{\boldsymbol{W}}_i^{\mathrm{T}} \boldsymbol{\Psi}_i - K_v \boldsymbol{s}_i^{\mathrm{T}} \boldsymbol{s}_i + \frac{1}{\eta_i} tr(\tilde{\boldsymbol{W}}_i^{\mathrm{T}} \dot{\tilde{\boldsymbol{W}}}_i) + \frac{1}{2} \left\| \xi_i \boldsymbol{s}_i \right\|^2 \\ &= -\left(K_v - \frac{1}{2} \xi_i^2 \right) \left\| \boldsymbol{s}_i \right\|^2 + \boldsymbol{s}_i^{\mathrm{T}} \tilde{\boldsymbol{W}}_i^{\mathrm{T}} \boldsymbol{\Psi}_i + \frac{1}{\eta_i} tr(\tilde{\boldsymbol{W}}_i^{\mathrm{T}} \dot{\tilde{\boldsymbol{W}}}_i) \end{aligned} \tag{25}$$

Substituting (17) into (25), then we know

$$\dot{H} \le -\varepsilon_1 \left\| \boldsymbol{s}_i \right\|^2 \le 0 \tag{26}$$

According to (23), and we can further get

$$\dot{V} \le \frac{1}{2} \gamma_i^2 \left\| \boldsymbol{\varepsilon}_i \right\|^2 - \frac{1}{2} \left\| \boldsymbol{z}_i \right\|^2 \tag{27}$$

5. Simulation Research

In this section, a simulation research is carried out to validate the effectiveness of the proposed distributed containment controllers. We choose four 2-DOF robots as the followers, and they are labeled as F1, F2, F3 and F4 respectively; three dynamic leaders, and they are labeled as L1, L2 and L3 respectively. The directed graph that characterizes the interaction among the followers and the leaders is shown in Figure 2.

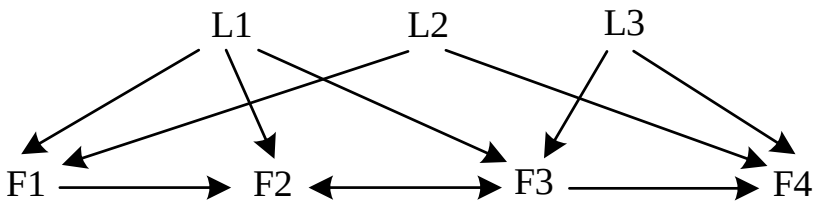

Figure 2. The Directed Graph that Characterizes the Interaction Among the Followers and the Leaders

Each follower has two cameras behind the end-effector, and all the followers have the same structure as shown in Figure 3.

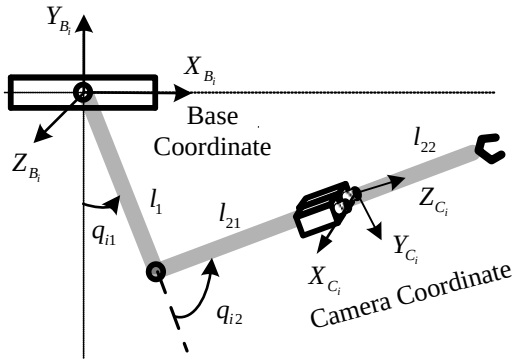

Figure 3. System Diagram of one Follower

In this section, the dynamic characteristics of the four followers are assumed to be the same, and the inertia matrix $\boldsymbol{M}_i(\boldsymbol{q}_i)$, the centripetal forces and Coriolis torques $\boldsymbol{C}_i(\boldsymbol{q}_i, \dot{\boldsymbol{q}}_i)$,

and the gravitational torques $\boldsymbol{G}_i(\boldsymbol{q}_i)$ are given by

$$\begin{cases} \boldsymbol{M}_i(\boldsymbol{q}_i) = \begin{bmatrix} 2.91 + 0.42\cos q_{i2} & 0.52 + 0.21\cos q_{i2} \\ 0.52 + 0.21\cos q_{i2} & 0.52 \end{bmatrix} \\ \boldsymbol{C}_i(\boldsymbol{q}_i, \dot{\boldsymbol{q}}_i) = \begin{bmatrix} -0.21\sin(q_{i2})\dot{q}_{i2} & -0.21\sin(q_{i2})(\dot{q}_{i1} + \dot{q}_{i2}) \\ 0.21\sin(q_{i2})\dot{q}_{i1} & 0 \end{bmatrix} \\ \boldsymbol{G}_i(\boldsymbol{q}_i) = \begin{bmatrix} 41.88\sin(q_{i1}) + 4.58\sin(q_{i1} + q_{i2}) \\ 4.58\sin(q_{i1} + q_{i2}) \end{bmatrix} \end{cases}$$

According to the direction relations between the camera coordinate system and the base coordinate system in Figure 3, then we have

$$\begin{cases} \boldsymbol{J}_A = \begin{bmatrix} l_{21}\cos(q_{i1} + q_{i2}) + l_1\cos q_{1i} & l_{21}\sin(q_{i1} + q_{i2}) + l_1\sin q_{i1} & 0 & 0 & 0 & 1 \\ l_{21}\cos(q_{i1} + q_{i2}) & l_{21}\sin(q_{i1} + q_{i2}) & 0 & 0 & 0 & 1 \end{bmatrix}^{\mathrm{T}} \\ \boldsymbol{T}(\boldsymbol{q}_i) = \begin{bmatrix} 0 & -\sin(q_{i1} + q_{i2}) & 0 \\ 0 & \cos(q_{i1} + q_{i2}) & 0 \\ -1 & 0 & 1 \end{bmatrix}, \quad \boldsymbol{R}_{B_i}^{C_i} = \begin{bmatrix} 0 & 0 & 1 \\ -\cos(q_{1i} + q_{2i}) & -\sin(q_{1i} + q_{2i}) & 0 \\ \sin(q_{1i} + q_{2i}) & \cos(q_{1i} + q_{2i}) & 0 \end{bmatrix} \end{cases}$$

Take the base coordinate system of F1 as the world coordinate system of the whole system, and the initial joint angles of the four followers are chosen as: $\boldsymbol{q}_1(0) = \boldsymbol{q}_2(0) = \left[240^\circ, -150^\circ\right]^{\mathrm{T}}$, $\boldsymbol{q}_3(0) = \boldsymbol{q}_4(0) = \left[-60^\circ, 150^\circ\right]^{\mathrm{T}}$; the initial coordinates of each robot are chosen as: $\mathrm{L1}(0) = [0.66,\ 0.38]^{\mathrm{T}}$, $\mathrm{L2}(0) = [0.56,\ 0.28]^{\mathrm{T}}$, $\mathrm{L3}(0) = [0.56,\ 0.48]^{\mathrm{T}}$, $\mathrm{F1}(0) = [0.36,\ 0.23]^{\mathrm{T}}$, $\mathrm{F2}(0) = [0.31,\ 0.33]^{\mathrm{T}}$, $\mathrm{F3}(0) = [0.31,\ 0.43]^{\mathrm{T}}$, $\mathrm{F4}(0) = [0.36,\ 0.53]^{\mathrm{T}}$.

Figure 4 is the trajectories of the four followers in the X-Y plane of the world coordinate system. In which the black circles denote the three dynamic leaders, the black triangle is the convex hull, and the small squares denote the four followers. Figure 5 describes the position curves of the four followers in each moment. As can be clearly seen from the two figures: 1. all followers can converge to the convex hull spanned by the leaders ultimately, although the leaders' information is available to only a portion of the followers; 2. there does not exist path crossing and overlapping phenomenon among the followers in the entire movement process, and then avoid the collision with each other under the action of the proposed control strategy.

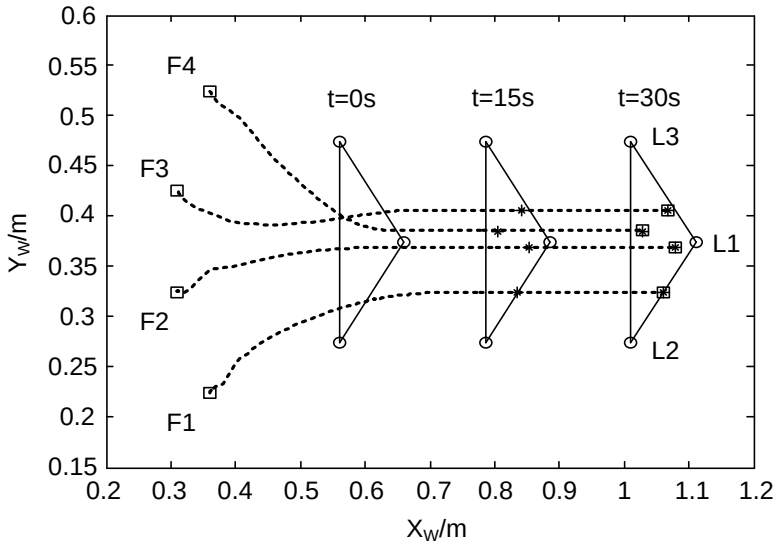

Figure 4. Trajectories of the Followers with the Dynamic Leaders

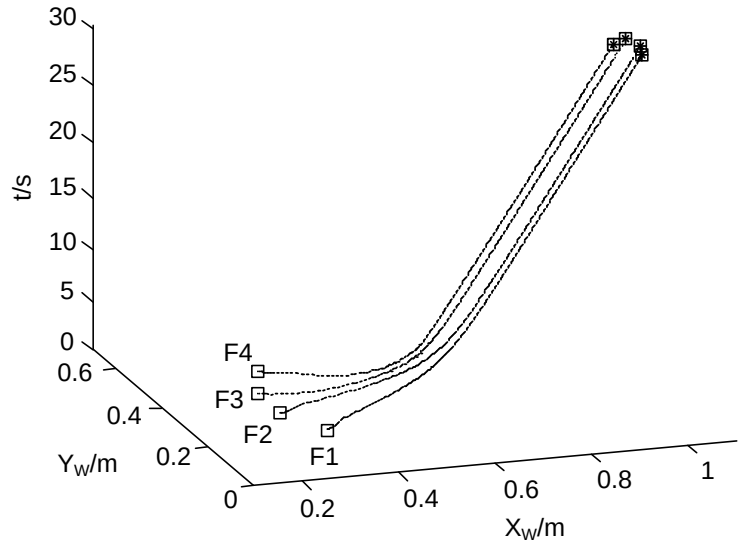

Figure 5. Position Curves of the Four Followers in Each Moment

Figure 6 shows the changing curves of the pseudo depth variable. The results illustrate that the value of the variable σ_i increases gradually with the decreases of the distance to the target points, i.e., its value is larger, the distance between the target point and the camera is closer, and can converge to the same value eventually until the four followers track their target points.

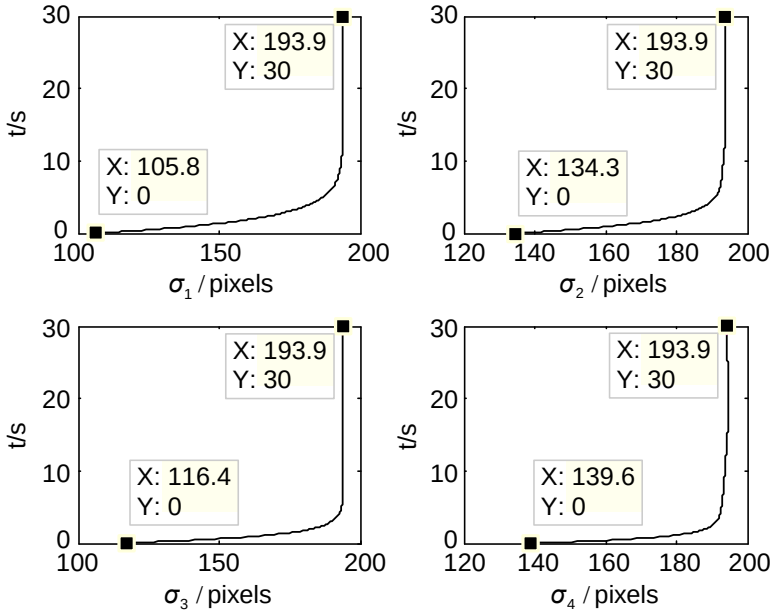

Figure 6. Curves of Pseudo Depth Variable

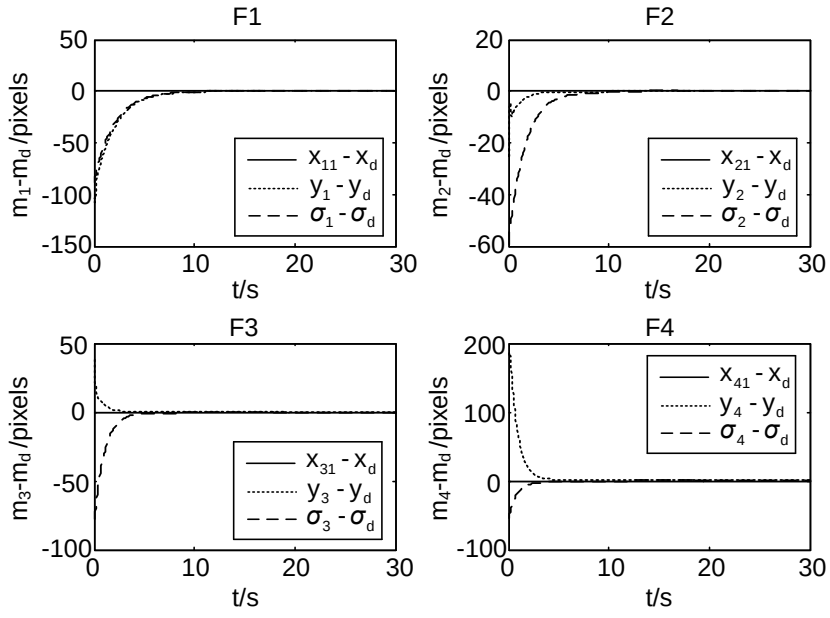

Figure 7. The Errors of the Four Target Points in the Image Plane Coordinate System

Figure 7 shows the error curves of the four target points in the image plane. It can be seen that each follower move to the desired location of target point in the image plane within 10 seconds, and the distributed containment control for multi-robot system based on binocular visual is realized.

6. Conclusion

In this paper, the distributed containment control problem is investigated based on

binocular vision system. Firstly, the topological relationship among the robots is built by using the directed graph, and a kind of binocular visual servo model is established for dynamic target points by introducing the pseudo depth variable, which makes all followers can determine their expected trajectories by using the status information of neighbor robots. Then, the distributed containment controllers are designed by using the sliding mode control method and RBF neural networks, which enhance the robust stability and improve the control precision of multi-robot system. Finally, a simulation research is carried out on seven 2-DOF robots, and results validate the followers can converge to the convex hull spanned by the dynamic leaders under the action of the proposed distributed containment controllers, and realize synchronization motion with the leaders ultimately.

Acknowledgements

This work was supported by Natural Science Foundation of Hebei Province under Grants No. F2012203111, Natural Science Youth Foundation of Higher Education of Hebei Province under Grants No. 2011139.

References

[1] W. Ren, R. Beard and E. M. Atkins, "Information consensus in multivehicle cooperative control", IEEE Control System Magazine, vol.27, no.2, **(2007)**, pp.71-82.
[2] Y. Cao and W. Ren, "Distributed coordinated tracking with reduced interaction via a variable structure approach", IEEE Transactions on Automatic Control, vol.57, no.1, **(2012)**, pp.33-48.
[3] Y. Cao, D. Stuart, W. Ren and Z. Meng, "Distributed containment control for multiple autonomous vehicles with double-integrator dynamics: algorithms and experiments", IEEE Transactions on Control Systems Technology, vol.19, no.4, **(2011)**, pp.929-938.
[4] R. O. Saber, J. A. Fax and R. M. Murray, "Consensus and cooperation in networked multi-agent systems", Proceedings of the IEEE, **(2007)**.
[5] Z. Y. Meng, Z. L. Lin and W. Ren, "Leader-follower swarm tracking for networked Lagrange systems", Systems & Control Letters, vol.61, no.1, **(2012)**, pp.117-126.
[6] J. Mei, W. Ren and G. F. Ma, "Distributed containment control for Lagrangian networks with parametric uncertainties under a directed graph", Automatica, vol.48, no.4, **(2012)**, pp.653-659.
[7] J. Mei, W. Ren, J. Chen and G. F. Ma, "Distributed adaptive coordination for multiple Lagrangian systems under a directed graph without using neighbors' velocity information", Automatica, vol.49, no.6, **(2013)**, pp.1723-1731.
[8] Y. H. Liu, H. S. Wang, C. Y. Wang and K. K. Lam, "Uncalibrated visual servoing of robots using a depth independent interaction matrix", IEEE Transactions on Robotics, vol.22, no.4, **(2006)**, pp.804-817.
[9] H. G. Li, M. Jin and L. Y. Zou, "A new binocular stereo visual servoing model", IEEE Pacific-Asia Workshop on Computational Intelligence and Industrial Application, **(2008)**, pp.461-465.
[10] B. Yang, H. G. Li, Z. B. Kang and H. L. Jiang, "Hamiltonian-based binocular visual servoing of camera-in-hand robotic systems", 4th International Conference on Modelling, Identification and Control, **(2012)**; Wuhan, China.
[11] B. Yang, H. G. Li, X. P. Sha and N. Shao, "An Immersion & invariance based speed observer for visual servoing", International Journal of Modelling, Identification and Control, vol.17, no.3, **(2012)**, pp.212-222.
[12] O. Nasisi and R. Carelli, "Adaptive servo visual robot control", Robotics and Autonomous Systems, vol.43, no.1, **(2003)**, pp.51-78.

Authors

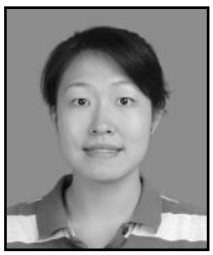

Nuan Shao, she is a Ph.D. candidate at the Institute of Electrical Engineering, Yanshan University, Qinhuangdao, PRC. Her research interests include robot visual control, visual tracking control of multi-robot system.

Huiguang Li, he now is a professor of automation department at Yanshan University and automation society executive direct of Hebei province. His research interests include robot visual control, sampled- data theory, microcomputer control system, embedded single chip microcomputer system, industry network controlling system.

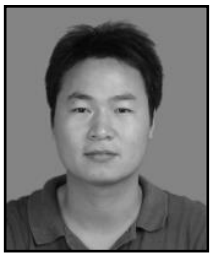

Le Liu, he is a Ph.D. candidate at the Institute of Electrical Engineering, Yanshan University, Qinhuangdao, PRC. His research interest covers include adaptive robust control theory and applications, variable structure control.

Guoyou Li, he now is a professor of automation department at Yanshan University Qinhuangdao, PRC. His research interests include servo control, robot fuzzy vision, artificial intelligence and applications.